Earth and Planetary Science Letters 454 (2016) 36–45

Contents lists available at ScienceDirect

Earth and Planetary Science Letters

www.elsevier.com/locate/epsl

A novel topographic parameterization scheme indicates that martian gullies display the signature of liquid water

Susan J. Conway [a,b,*], Matthew R. Balme [a]

[a] Department of Physical Sciences, Open University, Milton Keynes, MK7 6AA, UK
[b] Laboratoire de Planétologie et Géodynamique, UMR 6112, CNRS, Université de Nantes, 2 chemin de la Houssinière, BP 92205, 44322 Nantes Cedex 3, France [1]

ARTICLE INFO

Article history:
Received 16 February 2016
Received in revised form 13 July 2016
Accepted 23 August 2016
Available online 6 September 2016
Editor: C. Sotin

Keywords:
Mars
martian gullies
planetary geomorphology
geomorphometry

ABSTRACT

Martian gullies resemble gullies carved by water on Earth, yet are thought to have formed in an extremely cold ($< -50\,^{\circ}C$) and dry (humidity <100 precipitable micrometers) surface environment (cf. Mellon et al., 2004). Despite more than a decade of observations, no consensus has emerged as to whether liquid water is required to form martian gullies, with some recent studies favouring dry CO_2-driven processes. That this argument persists demonstrates the limitations of morphological interpretations made from 2D images, especially when similar-looking landforms can form by very different processes. To overcome this we have devised a parameterization scheme, based on statistical discriminant analysis and hydrological terrain analysis of meter-scale digital topography data, which can distinguish between dry and wet surface processes acting on a landscape. Applying this approach to new meter-scale topographic datasets of Earth, the Moon and Mars, we demonstrate that martian gullied slopes are dissimilar to dry, gullied slopes on Earth and the Moon, but are similar to both terrestrial debris flows and fluvial gullies. We conclude that liquid water was integral to the process by which martian gullies formed. Finally, our work shows that quantitative 3D analyses of landscape have great potential as a tool in planetary science, enabling remote assessment of processes acting on planetary surfaces.

1. Introduction

Gullies on Mars (Malin and Edgett, 2000) are widespread: they are concentrated in the mid-latitudes and can be found on steep slopes polewards of about 30° (Dickson et al., 2007). Global and hemispheric studies have revealed that mid-latitude gullies are located on slopes oriented towards the pole (Balme et al., 2006; Bridges and Lackner, 2006; Dickson et al., 2007; Harrison et al., 2015; Heldmann et al., 2007; Heldmann and Mellon, 2004; Kneissl et al., 2010; Marquez et al., 2005) while higher latitude examples have little, or no preferred orientation. The distribution and orientation of gullies are consistent with their formation at high obliquity, when pole-facing slopes receive maximum summer insolation. Together, this evidence led to the conclusion that gullies formed as water-rich debris flows (Costard et al., 2002).

However, increased insolation can also trigger dry mass wasting or destabilization of solid CO_2. Narrow channels observed on the Moon (Bart, 2007; Senthil Kumar et al., 2013; Xiao et al., 2013) and on the asteroid Vesta (Krohn et al., 2014; Scully et al., 2015) have been identified as analogues to martian gullies by some authors, yet these exist on airless bodies where erosion by traditional low-viscosity fluids is unlikely and whose surfaces are almost certainly completely dry. Hence, dry mass-wasting has been considered a potential formation mechanism for martian gullies. Some of the recent modifications observed in martian gullies, including new deposits and channel formation, have been found to occur at the time of year when CO_2 frost is subliming (Dundas et al., 2015, 2012, 2010; Raack et al., 2015; Vincendon, 2015). Therefore mechanisms involving gas release triggering granular flow (Cedillo-Flores et al., 2011; Pilorget and Forget, 2016), have been suggested for gully-formation. Theoretical modelling (Cedillo-Flores et al., 2011) predicts that sand-sized or smaller grains can be mobilized by CO_2 gas-sublimation under martian conditions but, unless there is a confining "lid" (Pilorget and Forget, 2016) on the flow, it rapidly converts from a gas-supported to a simple granular flow. Hence, we consider the visually-similar, gully-like granular flows observed on the Moon as suitable analogues for this process. We also con-

* Corresponding author at: Laboratoire de Planétologie et Géodynamique, UMR 6112, CNRS, Université de Nantes, 2 chemin de la Houssinière, BP 92205, 44322 Nantes Cedex 3, France.
E-mail address: susan.conway@univ-nantes.fr (S.J. Conway).
[1] Present address.

http://dx.doi.org/10.1016/j.epsl.2016.08.031
0012-821X/

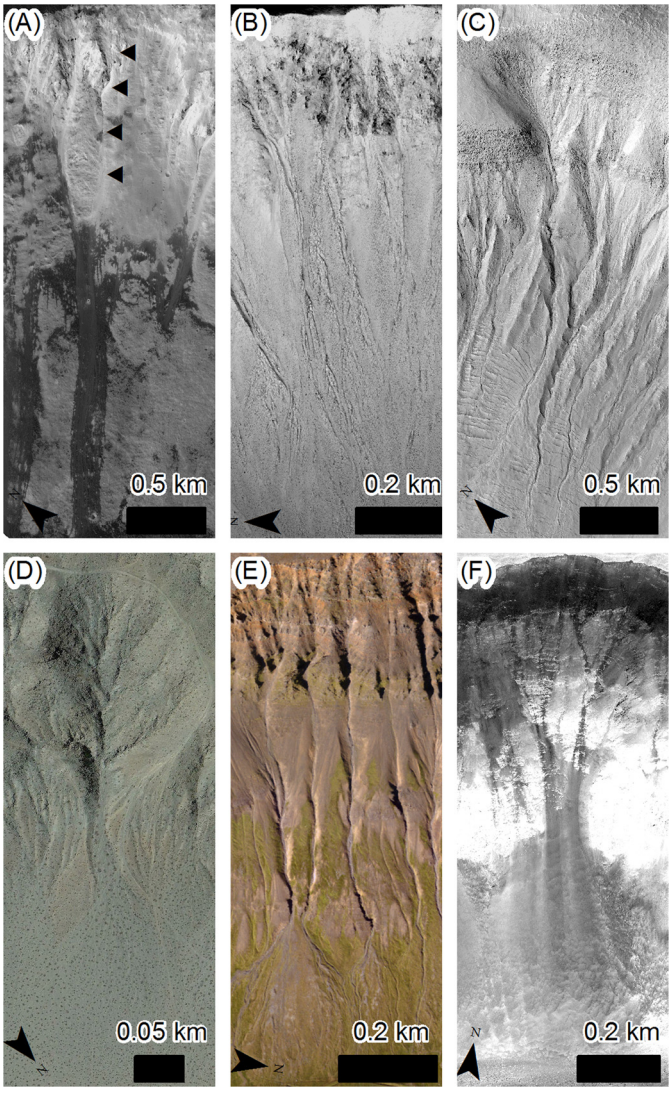

Fig. 1. Images of gullies on different planets. (A) Gullies on the Moon (arrows indicate the position of the "channel"), LROC image M151169370. Credit: NASA/Goddard Space Flight Center/Arizona State University. (B) Gullies on Mars in an unnamed crater NW of Lyot crater, HiRISE image ESP_027231_2340. Credit: NASA/JPL/University of Arizona. (C) Gullies in Palikir Crater on Mars, HiRISE image PSP_005943_1380. Credit: NASA/JPL/University of Arizona. (D) Ephemeral fluvial gully in Anderson Dry Lake, California on Earth – image from Google Earth. (E) Gullies on the eastern flank of Tindastóll Mountain, Iceland, Earth. Aerial image from NERC ARSF. (F) Talus slopes on the south-facing wall of Quebrada Camarones in the Atacama Desert northern Chile. Orthorectified GeoEye image at 0.5 m/pix.

sider mass-wasting deposits on Earth, in which water likely played a very minor role, as possible analogues for this process.

Here we go beyond plan-view comparisons of morphology, such as those illustrated in Fig. 1, by examining the three-dimensional properties of terrestrial, lunar and martian gullies. The inspiration for this study came from the delimitation of process-domains from digital elevation models of fluvial catchments on Earth. Montgomery and Foufoula-Georgiou (1993) calculated upslope drainage area and local slope for elevation data-pixels within fluvial catchments and showed that these properties follow a specific pattern in log–log space that depends on which processes were active in the catchment. They included process domains for fluvial and debris flow processes. We have further developed this approach by including other terrain attributes that can discriminate between processes such as cumulative area distribution, area distribution and 25 m downslope index, and by including dry granular flows (rockfalls, ravel and dry mass wasting) as an end-member process. Such hydrological analyses are not typically performed at the scale of the martian gullies (i.e. <5 km) because the data were not historically available. In an earlier study (Conway et al., 2011b) though, we showed that a qualitative comparison of slope-area and cumulative area distribution plots could discriminate between terrains dominated by debris flow, rockfall and fluvial processes on Earth at this scale. In the current study, we find that differences are also apparent in area distribution, and 25 m downslope index plots, as illustrated in Fig. 2. We extend our previous work by analyzing additional sites, including the Moon, and, more importantly, by performing a statistical analysis of the data.

2. Development of parameterization scheme

2.1. Hydrological analysis

The datasets used are fully described in the Supplementary material, summarized in Tables S1 and S2. We followed the same approach as Conway et al. (2011b) in generating the terrain attributes necessary for these analyses and a visual summary of these calculations is shown in Fig. S3. In brief, we used the multi-direction flow algorithm "dinf" which partitions flow into downslope neighbours in any direction (Tarboton, 1997). From these non-integer flow directions we calculated the (fractional) number of pixels located upstream of any given pixel, from which we calculated the uphill drainage area (Fig. S3D). Local slope (Fig. S3C) was calculated by taking the steepest of the eight triangular facets centred on the target pixel (Tarboton, 1997). The wetness index maps (Fig. S3A) were calculated by taking the natural logarithm of the ratio of drainage area to slope, excluding pixels with zero slope. We also calculated the flow directions and local slopes using the classic "d8" algorithm whereby flow is routed directly to a single downslope pixel, in one of the eight cardinal directions (O'Callaghan and Mark, 1984). From the d8 flow directions we calculated the distance downflow it is necessary to travel to achieve a given value of descent – the downslope index (Hjerdt et al., 2004) (Fig. S3F). If the value of descent is fixed at or near the DEM resolution, then the downslope index simply represents the steepest downstream slope. Conversely, if values are chosen which are of the same vertical scale as the feature being studied (~500 m for gullies), then within-feature detail is lost. We chose value of descent of 25 m, as a balance between these two end-members. These manipulations were performed using the freely available software packages TauDEM tools (Tarboton, 1997; Tesfa et al., 2011) and WhiteboxGAT (Lindsay, 2005).

2.2. Generating hydrological plots and parameters

The slope-area and cumulative area distribution plots were created following the method of Conway et al. (2011b). Briefly, the slope-area comprises the local slope and drainage area for every pixel plotted in log–log space, and these data are put into 0.05 wide log-drainage-area bins and for each bin the slope is averaged. Bins with less than 100 points are excluded to avoid bias of the mean by outlying datapoints, an approach employed commonly in other studies (e.g., Grieve et al., 2016). For the cumulative area distribution, the same bins are used, but the cumulative frequency for each bin is calculated. The non-cumulative area distribution plot is simply the histogram of the values of the logarithm of the drainage areas normalized by the maximum drainage area. The bin-width is 0.05. The curve is the kernel density estimation of the same distribution with a bandwidth of 0.05. The 25 m downslope index plot is similarly the histogram of the logarithm of the 25 m downslope index values with a 0.1 bin-width and the line is the corresponding kernel density with a bandwidth of 0.075.